

Quantum synchronization and entanglement of two qubits coupled to a driven dissipative resonator

O. V. Zhirov¹ and D. L. Shepelyansky^{2,3}¹*Budker Institute of Nuclear Physics, 630090 Novosibirsk, Russia*²*Laboratoire de Physique Théorique (IRSAMC), UPS, Université de Toulouse, F-31062 Toulouse, France*³*LPT (IRSAMC), CNRS, F-31062 Toulouse, France*

(Received 22 June 2009; published 24 July 2009)

Using method of quantum trajectories we study the behavior of two identical or different superconducting qubits coupled to a quantum dissipative driven resonator. Above a critical coupling strength the qubit rotations become synchronized with the driving field phase and their evolution becomes entangled even if two qubits may significantly differ from one another. Such entangled qubits can radiate entangled photons that opens new opportunities for entangled wireless communication in a microwave range.

DOI: [10.1103/PhysRevB.80.014519](https://doi.org/10.1103/PhysRevB.80.014519)

PACS number(s): 03.67.Bg, 03.67.Hk, 42.50.Lc, 85.25.-j

Recently, an impressive experimental progress has been reached in realization of a strong coupling regime of superconducting qubits with a microwave resonator.¹⁻⁵ The spectroscopy of exchange of one to few microwave photons with one,^{1,3} two,^{2,4} and even three⁵ superconducting qubits has been demonstrated to be in agreement with the theoretical predictions of the Jaynes-Cummings and Tavis-Cummings models⁶⁻⁸ even if certain nonlinear corrections have been visible. Thus the ideas of atomic physics and quantum optics find their promising implementations with superconducting macroscopic circuits leading also to achievement of single artificial-atom lasing in a microwave range.⁹

In comparison to quantum optics models⁶⁻⁸ a new interesting element of superconducting qubits is the dissipative nature of coupled resonator which opens new perspectives for quantum measurements.^{10,11} At the same time in the strongly coupled regime the driven dissipative resonator becomes effectively nonlinear due to interaction with a qubit that leads to a number of interesting properties.¹²⁻¹⁴ Among them is synchronization of qubit with a driven resonator phase¹⁴ corresponding to a single artificial-atom lasing realized experimentally in Ref. 9. The synchronization phenomenon has broad manifestations and applications in physics, engineering, social life, and other sciences¹⁵ but in the above case we have a striking example of quantum synchronization of a purely quantum qubit with a driven resonator having a semiclassical number of a few tens of photons.¹⁴ This interesting phenomenon appears above a certain critical coupling threshold¹⁴ and its investigation is now in progress.^{16,17}

Due to the experimental progress with two and three qubits²⁻⁵ it is especially interesting to study the case of two qubits where an interplay of quantum synchronization and entanglement opens a new field of interesting questions. The properties of entanglement for two atoms (qubits) coupled to photons in a resonator have been studied recently in the frame of Tavis-Cummings model within the rotating wave approximation (RWA).^{18,19} Compared to them we are interested in the case of dissipative driven resonator strongly coupled to qubits where RWA is not necessarily valid and where the effects of quantum synchronization between qubits and the resonator are of primary importance. In addition we consider also the case of different qubits which is rather un-

usual for atoms but is very natural for superconducting qubits.

In absence of dissipation the whole system is described by the Hamiltonian

$$\hat{H} = \hbar\omega_0(\hat{n} + 1/2) + \hbar\Omega_1\sigma_z^{(1)}/2 + \hbar\Omega_2\sigma_z^{(2)}/2 + g\hbar\omega_0(\sigma_x^{(1)} + \sigma_x^{(2)})(\hat{a} + \hat{a}^\dagger) + f \cos \omega t \cdot (\hat{a} + \hat{a}^\dagger), \quad (1)$$

where the first three terms represent photons in a resonator and two qubits, g term gives the coupling between qubits and photons, and the last term is the driving of resonator. In presence of dissipation the resonator dissipation rate is λ and its quality factor is assumed to be $Q = \omega_0/\lambda \sim 100$. The decay rate of qubits is supposed to be zero corresponding to a reachable experimental situation¹⁻⁵ where their decay rate is much smaller than λ . The driving force amplitude is expressed as $f = \hbar\lambda\sqrt{n_p}$, where n_p is a number of photons in a resonator at the resonance $\omega = \omega_0$ when $g = 0$. The whole dissipative system is described by the master equation for the density matrix $\hat{\rho}$ which has the standard form²⁰

$$\dot{\hat{\rho}} = -\frac{i}{\hbar}[\hat{H}, \hat{\rho}] + \lambda(\hat{a}\hat{\rho}\hat{a}^\dagger - \hat{a}^\dagger\hat{a}\hat{\rho}/2 - \hat{\rho}\hat{a}^\dagger\hat{a}/2). \quad (2)$$

The numerical simulations are done by the method of quantum trajectories²¹ with the numerical parameters and techniques described in Ref. 14.

To analyze the system properties we determine the spectral density of driven qubits defined as $S(\nu) = |\int dt \exp\{-i\nu t\} \text{Tr}\{\hat{\rho}[\sigma_x^{(1)} + \sigma_x^{(2)}]/2\}|^2$. Its dependence on system parameters for identical and different qubits is shown in Fig. 1. At small couplings g the spectrum of qubits $S(\nu)$ shows the lines at the internal qubit frequencies $\Omega_{1,2}$ but above a certain critical coupling strength $g > g_c$ the quantum synchronization of qubits with the driven resonator takes place and the unperturbed spectral lines are replaced by one dominant spectral line at the driving frequency with $\nu = \omega$ [Figs. 1(a) and 1(b)]. A similar phenomenon takes place for $g > g_c(f)$ when the strength of resonator driving $f \propto \sqrt{n_p}$ is increased [Figs. 1(c) and 1(d)]. Indeed, with the growth of n_p the number of photons in the resonator increases that leads to a stronger coupling between photons and qubits and eventual synchro-

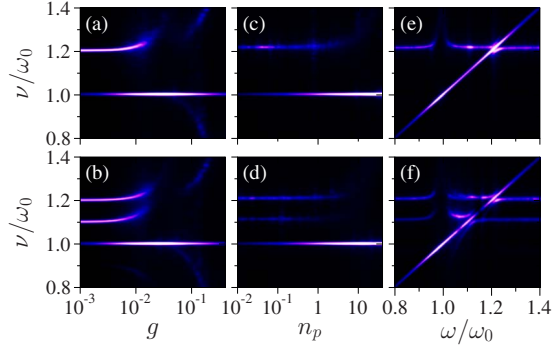


FIG. 1. (Color online) Spectral density $S(\nu)$ of two driven qubits as a function of system parameters for identical $\Omega_1/\omega_0 = \Omega_2/\omega_0 = 1.2$ (top row) and different $\Omega_1/\omega_0 = 1.1$, $\Omega_2/\omega_0 = 1.2$ (bottom row) qubits: (a) and (b) $n_p = 15$, $\omega/\omega_0 = 1$; (c) and (d) $g = 0.04$, $\omega/\omega_0 = 1$; and (e) and (f) $n_p = 15$, $g = 0.04$. Here and below $\lambda/\omega_0 = 0.02$.

nization. The synchronization of qubits with the resonator is also clearly seen from Figs. 1(e) and 1(f), where the spectral line of $S(\nu)$ follows firmly the variation in driving frequency ω . The striking feature of Fig. 1 is that even rather different qubits with significant frequency detunings $|\Omega_{1,2} - \omega_0| \gg \lambda$ become synchronized due to their coupling with the resonator getting the same lasing frequency $\nu \approx \omega$.

For a better understanding of this phenomenon we analyze the dependence of the average number of photons in the resonator $\langle n \rangle$ on driving frequency ω (see Fig. 2, top panels). It has three pronounced maxima which up to quantum fluctuations correspond to three values of the total spin component $S_z = \text{Tr}\{\rho[\sigma_z^{(1)} + \sigma_z^{(2)}]/2\}$ being close to the values $S_z = -1, 0, 1$ with the total spin $S = 1$ (triplet state) as it is clearly seen from the data shown in the middle panels of Fig. 2. The whole dependence of $\langle n \rangle$ on ω is well fitted by the resonance curves $n_{S_z} = n_p \lambda^2 / [4(\omega - \omega_0 - \Delta\omega_{S_z})^2 + \lambda^2]$ where

the frequency shift $\Delta\omega_{S_z}$ appears due to the effective Rabi frequency Ω_R which gives oscillations between the resonant states. The value of Ω_R is induced by the coupling between qubits and photons in Eq. (1) (Refs. 6–8) and can be approximated obtained as an average value of coupling that gives $\Omega_R = 2aS_z g \omega_0 \sqrt{(1 - \langle S_z \rangle^2)(n_{S_z} + 1)} \approx 2S_z a \Omega_{R0}$ with $\Omega_{R0} = g \omega_0 \sqrt{n_{S_z} + 1}$. This gives the frequency shift $\Delta\omega_{S_z} = d\Omega_R/dn_{S_z}$ which determines the resonant dependence $n_{S_z}(\omega)$ in a self-consistent way. Such a theory gives a good description of numerical data as it is shown in Fig. 2 (top panel) where the corresponding values of $\langle S_z \rangle$ are taken from the middle panel. The numerical coefficient a smoothly varies between 1.14 and 1.57 for $0.01 \leq g \leq 0.06$. This resonance dependence is similar to the one qubit case discussed in Ref. 14 but the effects of quantum fluctuations are larger due to mutual effective coupling between qubits via the dissipative resonator. On the basis of these estimates it is natural to assume that the quantum synchronization of a qubit with a driving phase takes place under the condition that the detuning is smaller than the typical value of Rabi frequency

$$|\Omega_{1,2} - \omega| < \Omega_{R0} = g \omega_0 \sqrt{n_{S_z} + 1} \approx g \omega_0 \sqrt{n_p + 1}. \quad (3)$$

This criterion assumes a semiclassical nature of photon field with the number of photons $n_p > 1$. Its structure is similar to the classical expression for the synchronization tongue which is proportional to the driving amplitude being independent of dissipation rate.¹⁵ The relation (3) determines the border for quantum synchronization $g_c \approx |\Omega_{1,2} - \omega| / \omega_0 \sqrt{n_p + 1}$.

The entanglement between qubits is characterized by concurrence C (see, e.g., the definition in Ref. 18). Its dependence on ω is shown in the bottom panels of Fig. 2. It is striking that the concurrence C can be close to unity not only for identical qubits but also for different qubits. Qualitatively, this happens due to synchronization of qubits induced by the resonator driving which makes them “quasi-identical” and allows to create the entangled state with $S_z = 0$.

To understand the properties of the system in a better way we show the time evolution of its characteristics along a typical quantum trajectory in Fig. 3. Average number of photons in the resonator $\langle n \rangle$ shows tunneling transitions between two metastable states induced by quantum fluctuations (top panels). There are no transitions to the third metastable state, seeing in Fig. 2 with three resonant curves, but we had them on longer times or for other realizations of quantum trajectories (see also Fig. 4). The lifetime inside each metastable state is on the order of thousands of driving periods and the change in $\langle n \rangle$ is macroscopically large (about a ten of photons). The transition leads also to a change in total spin polarization components $S_{x,y,z} = \text{Tr}\{\rho[\sigma_{x,y,z}^{(1)} + \sigma_{x,y,z}^{(2)}]/2\}$ (middle panels). It takes place on a relatively short time scale $\sim 1/\lambda$. The transition also generates emergence or death of concurrence C (or entanglement) which happens on the same time scale $1/\lambda$ (bottom panels). Naturally, C is maximal when $S_x \approx 0$. Remarkably, during long-time intervals C remains to be close to its maximal value $C = 1$ even for the case of different qubits. We attribute this phenomenon to synchronization of two qubits by driven resonator.

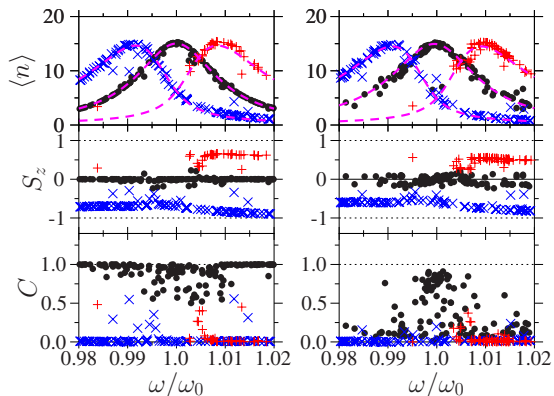


FIG. 2. (Color online) The average quantities of number of photons in the resonator $\langle n \rangle$ (top), total spin polarization S_z (middle), and the concurrence of two qubits C (bottom) vs the driving frequency ω . Left: identical qubits with $\Omega_1/\omega_0 = \Omega_2/\omega_0 = 1.2$, right: different qubits with $\Omega_1/\omega_0 = 1.1$, $\Omega_2/\omega_0 = 1.2$. Other parameters are $\lambda/\omega_0 = 0.02$, $n_p = 15$, and $g = 0.04$. Symbols mark the values of the total spin S_z : $S_z > 0.2$ (red/gray +), $|S_z| \leq 0.2$ (black dots), and $S_z < -0.2$ (blue/black ×). Dashed curves on top panels show the resonance dependence $n_{S_z}(\omega)$ (see text) with the resonance shift $\Delta\omega_{S_z} = 1.35S_z g \omega_0 \sqrt{(1 - \langle S_z \rangle^2)/(n_{S_z} + 1)}$.

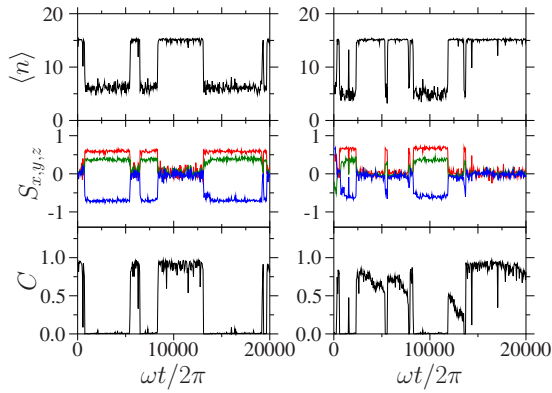


FIG. 3. (Color online) Time evolution of system quantities: average photon number $\langle n \rangle$ (top); components of total spin polarization $S_{x,y,z}$ (middle) where x,y,z components correspond to red, green, and blue colors [curves from top to bottom at $\omega t/2\pi=1.5 \times 10^4$ (left) and 10^4 (right)]; concurrence C (bottom). Left: two identical qubits with $\Omega_{1,2}/\omega_0=1.2$, right: two different qubits with $\Omega_1/\omega_0=1.1$ and 1.2 . Data are shown at stroboscopic moments of time with driving phase $\varphi = \omega t \pmod{2\pi} = 0$. Here $\omega/\omega_0=1$, other parameters are as in Fig. 2.

To display and characterize this phenomenon in more detail we determine the phases of oscillator and qubits via relations $\phi_0 = \arctan(\text{Im}(\hat{a})/\text{Re}(\hat{a}))$ and $\phi_{1,2} = \arctan(\langle s_x^{(1,2)} \rangle / \langle s_y^{(1,2)} \rangle)$, respectively. The variation in these phases with the driving phase $\varphi = \omega t \pmod{2\pi}$ is shown in Fig. 4 for different

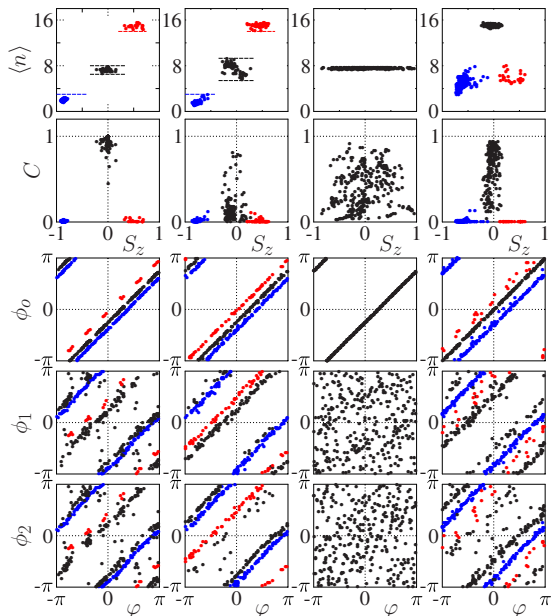


FIG. 4. (Color online) Rows from top to bottom: average photon number $\langle n \rangle$ vs S_z ; concurrence C vs S_z ; and resonator phase ϕ_0 and qubits phases $\phi_{1,2}$ vs the driving force phase φ . Columns from left to right: (i) two identical qubits with $\Omega_{1,2}/\omega_0=1.2$, $g=0.04$, (ii)–(iii) two different qubits, with $\Omega_1/\omega_0=1.1$, $\Omega_2/\omega_0=1.2$, $g=0.04$ and 0.001 , all three columns correspond to driving frequency $\omega/\omega_0=1.01$. The last column (iv) shows data for two different frequency qubits with $\Omega_1/\omega_0=1.1$, $\Omega_2/\omega_0=1.2$, and $g=0.04$ but the driving frequency $\omega/\omega_0=1$ [cf. (ii)]. Colors of points are explained in the text. Other parameters of simulations are: $\lambda/\omega_0=0.02$, $n_p=15$.

values of system parameters corresponding to columns (i), (ii), (iii), and (iv). For identical qubits [column (i)] the numerical data obtained along one long quantum trajectory form three well-defined groups of points in the plane of $\langle n \rangle$ and S_z (data are taken at stroboscopic moments of time t with a certain frequency comparable but incommensurate with ω to sweep all phases φ). It is convenient to mark these groups by three different colors corresponding to small (blue or dark gray), medium (black), and large (red or light gray) values of $\langle n \rangle$ (the groups are also marked by horizontal lines). Such a classification shows that three groups have not only distinct values of $\langle n \rangle$ but also three distinct locations in concurrence C and spin S_z . Also these groups show three lines in the phase plane for oscillator (ϕ_0, φ) and for each qubit ($\phi_{1,2}, \varphi$). Of course, due to quantum fluctuations there are certain fluctuations for qubit phases but the linear dependence between phases is seen very clearly, thus showing the quantum synchronization of system phases with the driving phase φ . Physically, the three groups correspond to the three triplet states of total spin $S=1$. Indeed, for identical qubits the states with total spin values $S=1$ and 0 are decoupled and the dynamics of $S=0$ state is trivial [see Eq. (1)]. For different qubits [columns (ii) and (iv)] the quantum synchronization between phases is also clearly seen even if two qubits have rather different frequency detunings. For the case (ii) the concurrence is smaller compared to the case of identical qubits (i) but by a change in driving frequency ω it can be increased [see the case (iv)] to the values as high as for identical qubits in (i). We note that for different qubits [e.g., for (ii)] there is a visible splitting of the middle group of black points in the $(\langle n \rangle, S_z)$ plane which corresponds to states with mixed components of total spin $S=1$ and 0 : indeed, for different qubits the coupling between the states $S=1$ and 0 is nonzero and such transitions can take place (however, on the phase planes the splitting of black points is too weak to be seen in presence of quantum fluctuations). Of course, the numerical data show the presence of quantum fluctuations around straight lines in the phase planes. Nevertheless, this regime of quantum synchronization at $g > g_c$ is qualitatively different from the regime below the synchronization border $g < g_c$ where the points are completely scattered over the whole phase plane [column (iii)]. In this regime (iii) the qubits rotate independently from the resonator which stays at fixed number of photons. In contrast, for $g > g_c$ two qubits move in quantum synchrony during a large number of oscillations being entangled. A single superconducting qubit lasing has been already achieved in experiments.⁹ Our theoretical studies show that such two qubits, which in practice are always nonidentical, can be made entangled and produce lasing in synchrony with each other. Being entangled such qubits can radiate entangled photons in a microwave range. Therefore, the experiments similar to Ref. 9 but with two single-atoms lasing would be of great interest for entangled microwave photons generation.

In the above studies we made a number of simplifying assumptions. We assumed that the qubit decay rate Γ_q is much smaller than the typical oscillation and nonlinear frequencies of qubits. Also it is supposed that it is smaller than the resonator decay rate $\Gamma_q \ll \lambda$. In addition, there is no external dephasing of qubits. In spite of these points we think

that the presented results are interesting and reserve experimental tests. Indeed, lifetimes of qubits as long as few microseconds are now within experimental reach (see, e.g., Refs. 1–5 and 22). This is, in principle, sufficiently large compared to times of nonlinear frequency shifts which are close to GHz range. Also, hopefully, a small dephasing rates of qubits compared to nonlinear coupling frequencies can be accessible experimentally. Indeed, the spectroscopy of qubits allows now to observe nonlinear shifts induced by resonator coupling. In this regime of strong coupling between qubits and resonator²² the quantum synchronization of qubits can be reached experimentally if the synchronization criterion (3) is fulfilled. In this regime the qubits will be entangled. This is a necessary condition to generate entangled microwave photons. Of course, there are still other conditions to be reached to obtain significant generation efficiency of such photons:

the emission properties of a cavity and its linewidth should be analyzed in detail. But the main element of creation of entangled qubits is shown to be theoretically possible that paves the way for future experimental progress to entangled microwave photons generation.

In conclusion, our numerical simulations show that even two different superconducting qubits can move in quantum synchrony induced by coupling to a driven dissipative resonator, which can make them entangled. Such entangled qubits can radiate entangled microwave photons that open interesting opportunities for wireless entangled communication in a microwave domain.

The work is funded by EC project EuroSQIP, French ANR projects MICONANO and NANOTERRA, and RAS grant “Fundamental problems of nonlinear dynamics.”

-
- ¹A. Wallraff, D. I. Schuster, A. Blais, L. Frunzio, R. S. Huang, J. Majer, S. Kumar, S. M. Girvin, and R. J. Schoelkopf, *Nature* (London) **431**, 162 (2004).
- ²J. Majer, J. M. Chow, J. M. Gambetta, J. Koch, B. R. Johnson, J. A. Schreier, L. Frunzio, D. I. Schuster, A. A. Houck, A. Wallraff, A. Blais, M. H. Devoret, S. M. Girvin, and R. J. Schoelkopf, *Nature* (London) **449**, 443 (2007).
- ³J. M. Fink, M. Göppl, M. Baur, R. Bianchetti, P. J. Leek, A. Blais, and A. Wallraff, *Nature* (London) **454**, 315 (2008).
- ⁴S. Filipp, P. Maurer, P. J. Leek, M. Baur, R. Bianchetti, J. M. Fink, M. Göppl, L. Steffen, J. M. Gambetta, A. Blais, and A. Wallraff, *Phys. Rev. Lett.* **102**, 200402 (2009).
- ⁵J. M. Fink, R. Bianchetti, M. Baur, M. Goeppel, L. Steffen, S. Filipp, P. J. Leek, A. Blais, and A. Wallraff, arXiv:0812.2651 (unpublished).
- ⁶E. T. Jaynes and F. W. Cummings, *Proc. IEEE* **51**, 89 (1963).
- ⁷M. Tavis and F. W. Cummings, *Phys. Rev.* **170**, 379 (1968).
- ⁸M. O. Scully and M. S. Zubairy, *Quantum Optics* (Cambridge University Press, Cambridge, 1997).
- ⁹O. Astafiev, K. Inomata, A. O. Niskanen, T. Yamamoto, Yu. A. Pashkin, Y. Nakamura, and J. S. Tsai, *Nature* (London) **449**, 588 (2007).
- ¹⁰A. N. Korotkov, *Phys. Rev. B* **60**, 5737 (1999); **67**, 235408 (2003); A. N. Korotkov and D. V. Averin, *ibid.* **64**, 165310 (2001).
- ¹¹M. Sarovar, H.-S. Goan, T. P. Spiller, and G. J. Milburn, *Phys. Rev. A* **72**, 062327 (2005).
- ¹²J. Hauss, A. Fedorov, C. Hutter, A. Shnirman, and G. Schön, *Phys. Rev. Lett.* **100**, 037003 (2008).
- ¹³J. Gambetta, A. Blais, M. Boissonneault, A. A. Houck, D. I. Schuster, and S. M. Girvin, *Phys. Rev. A* **77**, 012112 (2008).
- ¹⁴O. V. Zhirov and D. L. Shepelyansky, *Phys. Rev. Lett.* **100**, 014101 (2008).
- ¹⁵A. Pikovsky, M. Rosenblum, and J. Kurths, *Synchronization: A Universal Concept in Nonlinear Sciences* (Cambridge University Press, Cambridge, United Kingdom, 2001).
- ¹⁶S. André, V. Brosco, A. Shnirman, and G. Schön, *Phys. Rev. A* **79**, 053848 (2009).
- ¹⁷A. Ashhab, J. R. Johansson, A. M. Zagoskin, and F. Nori, *New J. Phys.* **11**, 023030 (2009).
- ¹⁸T. E. Tessier, I. H. Deutsch, A. Delgado, and I. Fuentes-Guridi, *Phys. Rev. A* **68**, 062316 (2003).
- ¹⁹A. Retzker, E. Solano, and B. Reznik, *Phys. Rev. A* **75**, 022312 (2007).
- ²⁰U. Weiss, *Dissipative Quantum Mechanics* (World Scientific, Singapore, 1999).
- ²¹T. A. Brun, I. C. Percival, and R. Schack, *J. Phys. A* **29**, 2077 (1996); T. A. Brun, *Am. J. Phys.* **70**, 719 (2002).
- ²²M. Devoret, S. Girvin, and R. Schoelkopf, *Ann. Phys. (Leipzig)* **16**, 767 (2007).